3254 *Biochemistry* **2010,** *49,* 3254–3260
DOI: 10.1021/bi902134p

BIOCHEMISTRY
including biophysical chemistry & molecular biology
Article

Mechanisms of Enzymatic Degradation of Amyloid β Microfibrils Generating Nanofilaments and Nanospheres Related to Cytotoxicity[†]

Keiji Numata and David L. Kaplan*

Department of Biomedical Engineering, Tufts University, 4 Colby Street, Medford, Massachusetts 02155

Received December 11, 2009; Revised Manuscript Received February 7, 2010

ABSTRACT: Amyloid β (Aβ) fibrils are found in the brain tissue of persons with Alzheimer's disease (AD), where they accumulate as plaques. One way to reduce the level of accumulation of Aβ in the brain and potentially treat AD is with Aβ-degrading enzymes such as neprilysin (NEP) and insulin-degrading enzyme (IDE). However, enzymatic responses and degradation mechanisms of Aβ fibrils (crystalline-state Aβ) have not been investigated, particularly with respect to how to avoid cytotoxicity of the degradation products to neuronal cells. Thus, insight into mechanisms of enzymatic degradation of Aβ fibrils would be instructive as a route to elucidating different structural features related to degradation and to cytotoxicity. We report mechanisms of enzymatic degradation of Aβ with cross-β structures and show the series of steps involved in the digestion of Aβ microfibrils to nanospheres or nanofilaments by protease XIV or α-chymotrypsin, respectively. These degradation products, which contained almost the same secondary structures, exhibited different cytotoxicities, indicating that relationships between nanoassembled structures and cytotoxicity of Aβ peptides are more significant than the β-sheet content. In addition, the enzymatic digestion at the Lys28 loop region linking the two β-sheets in Aβ fibrils is suggested as a key target related to cytotoxicity, a feature that can be selectively targeted on the basis of the choice of protease.

Protein fibril formation, which is induced by the secondary structure conversion of proteins, plays a central neuropathological role in human diseases, including amyloidoses such as Alzheimer's disease (AD)[1] (*1*, *2*). Amyloids are generally described as stacked β-sheet structures aligned perpendicular to the fibril axis, known as cross-β sheets, and are often based on hydrophobic interactions between the side chains (*3*, *4*). Amyloid β (Aβ) fibrils are found in the brain tissue of persons with AD, where they accumulate as plaques. Monomers, intermediates (oligomers), and fibrils of Aβ peptides with different molecular weights have been investigated for neurotoxicity, and recently, a spherical amyloid intermediate 15−35 nm in diameter, which had predominantly β-sheet structures, demonstrated higher toxicity than Aβ monomers and fibrils (*5*). The C-terminus of Aβ(1−42) was also reported to be critical for the seeding of amyloid formation (*6*). Additionally, a cell viability screen with Aβ(*x*−42) fragments (*x* = 28−39) identified that Aβ(31−42) and Aβ-(39−42) inhibited Aβ-induced cell death and stabilized Aβ(1−42) in nontoxic oligomers, whereas Aβ(28−42) was highly toxic likely due to the presence of Lys28 at the N-terminus. This lysine increases the positive charge at physiologic pH relative to those of the other Aβ fragments (*7*). Furthermore, Met35 of Aβ(1−42) was reported to be critical to both oxidative stress and neurotoxic properties of native Aβ peptides (*8*, *9*). However, the structural mechanisms for amyloid peptides, such as the nanoassembly of Aβ fragments, related to neurotoxicity have not been clarified.

Anti-amyloid immunotherapy, which is a promising anti-amyloid approach for AD therapeutics, has been shown to be effective in animal models and reduced the plaque burden in clinical trials (*10*−*12*). Another way to reduce the level of accumulation of Aβ in the brain is with the use of Aβ-degrading enzymes such as neprilysin (NEP) and insulin-degrading enzyme (IDE) (*13*−*16*). NEP is synthesized as a membrane-bound protein and regulated in neurons by the protein nicastrin, a component of the γ-secretase complex that performs a necessary step in processing amyloid precursor protein to Aβ (*17*). The majority of IDE is present in the cytosol, with smaller amounts present in mitochondria, peroxisomes, and the plasma membrane, whereas a small fraction of IDE is also trafficked to the extracellular space to interact with known substrates of IDE, such as insulin and Aβ (*16*, *18*). The catalytic parameters and possible sites of cleavage of soluble Aβ by IDE have already been studied (*19*). For the practical use of these enzymes in treating AD, they would need to be activated in their Aβ-degrading activity whereas minimally affecting their activity on the other substrates (*20*). However, the biological activity of the degradation products related to AD has not been clarified in relation to AD therapeutics. Furthermore, enzymatic specificities of NEP and IDE against crystalline peptides, which are not water-soluble, have not been investigated as a route for treatment of AD. Several proteolytic enzymes have been used to digest β-sheet proteins, with protease XIV thought to exhibit high activity toward β-sheet structures (*21*−*25*). In contrast, α-chymotrypsin

[†]This work has been supported by grants from the National Institutes of Health and the National Science Foundation (D.L.K.). K.N. was supported by a Japan Society for the Promotion of Science Postdoctoral Fellowship for Research Abroad.

*To whom correspondence should be addressed: Tufts University, 4 Colby St., Medford, MA 02155. Phone: (617) 627-3251. Fax: (617) 627-3231. E-mail: david.kaplan@tufts.edu.

[1]Abbreviations: Aβ, amyloid β; AD, Alzheimer's disease; MTS, 3-(4,5-dimethylthiazol-2-yl)-5-(3-carboxymethoxyphenyl)-2-(4-sulfophenyl)-2*H*-tetrazolium; NEP, neprilysin; IDE, insulin-degrading enzyme; MFTIR, microscopic Fourier transform spectroscopy; OM, optical microscopy; AFM, atomic force microscopy; CD, circular dichroism; MALDI-TOF, matrix-assisted laser desorption ionization time-of-flight mass spectrometry; ACN, acetone nitride; TFA, trifluoroacetic acid; MWCO, molecular weight cutoff.

 Published on Web 03/02/2010

can digest the less crystalline regions of the assembled protein structures but does not degrade the β-sheet crystals (*21*−*24*). Possible cleavage sites and amino acid sequences for protease XIV and α-chymotrypsin have also been investigated (*26*−*28*).

The goal of this study was to examine how proteolytic enzymes in addition to NEP and IDE interact with cross-β Aβ fibrils with in-register parallel β-sheet structures. With this insight, new views of mechanisms related to neurotoxicity of nanoassemblies of Aβ fragments can be gained for new insights into AD therapeutics via enzymatic treatments.

EXPERIMENTAL PROCEDURES

Preparation of Aβ Fibrils. The Aβ(1−42) peptide was purchased from Sigma-Aldrich (St. Louis, MO) and 5 mM Aβ(1−42) peptide dissolved in DMSO and then sonicated for 10 min at 37 °C, according to literature methods (*7*, *29*). The Aβ(1−42) peptide solution was diluted to 100 μM with 10 mM HCl, subsequently sonicated for 30 min, and filtered with a Microncon 10000 MWCO (Millipore Corp., Billerica, MA). After incubation of the Aβ(1−42) peptide solution at 37 °C for 2 days, Aβ fibrils were obtained. The solution including the fibrils was deposited on a gold-spattered substrate, and the deposited substrates were used as samples for microscopic Fourier transform spectroscopy (MFTIR), optical microscopy (OM), and atomic force microscopy (AFM).

Observation and Characterization of Aβ Fibrils. MFTIR measurements of Aβ microfibril crystals on gold substrates were taken with a JASCO FT/IR-6200 instrument equipped with an IRT-5000 infrared microscope. MFTIR spectra were recorded at a resolution 4 cm^{-1} with a liquid nitrogen-cooled mercury−cadmium−telluride [MCT(Hg1-XCdXTe)] detector (reflection mode). The fibrils on substrates were observed by AFM (Veeco, Nanoscope III) in air. A 225 μm long silicon cantilever with a spring constant of 3 N/m was used in tapping mode. The lateral dimensions from AFM measurements include errors due to the convolution effect, while the thickness measured by AFM should be more precise. Considering the geometry of the cantilever tip and object (Aβ fibrils in this study), the calibration of tip convolution effect was conducted, yielding true dimensions of the object using the method reported previously (*30*).

Enzymatic Degradation. The Aβ fibrils were treated with proteolytic enzymes, protease XIV (Sigma-Aldrich), and α-chymotrypsin (Sigma-Aldrich) for 24 h and with neprilysin (NEP) and insulin-degrading enzyme (IDE) (R&D Systems Inc., Minneapolis, MN) for 48 h in a 0.1 M phosphate buffer solution (pH 7.4) at 37 °C. The concentration of protease XIV and α-chymotrypsin was set at 100 μg/mL, and that of NEP and IDE was set at 50 μg/mL, according to the literature methods (*20*, *31*).

Matrix-Assisted Laser Desorption Ionization Time-of-Flight Mass Spectrometry (*MALDI-TOF*). A Micro Flex mass spectrometer (Bruker Daltonik GmbH, Leipzig, Germany) was used to determine the molecular weights of degradation products. The solution containing Aβ peptides (approximately 1 μg/mL) was mixed with a saturated sinapic acid (Sigma-Aldrich) solution containing acetone nitride (ACN) and 0.1% trifluoroacetic acid (TFA) (1:2 ACN:TFA ratio). Each sample was measured in the molecular weight range of 20−5000.

Estimation of Enzymatic Digestion. Estimations of enzymatic digestion patterns of an Aβ(1−42) peptide were performed as follows. Protease XIV was regarded as a serine esterase to digest preferentially peptide bonds to the C-terminal side of the following amino acids, Trp, Tyr, Phe, Leu, Met, His, Lys, and Arg. Also, α-chymotrypsin was used as a serine esterase to digest preferentially peptide bonds to the C-terminal side of the following amino acids, Trp, Tyr, Phe, Leu, Met, and His. The digestion behavior by the enzymes was based on the literature (*26*−*28*).

Circular Dichroism (*CD*). CD spectra of Aβ microfibrils before and after enzymatic degradation for 24 or 48 h were recorded at 37 °C using an AVIV model 410 spectrometer and AVIV 410 CD Instrument (AVIV Biomedical Inc., Lakewood, NJ). CD spectra were recorded at a speed of 12 nm/s and a resolution of 1 nm. Spectra of enzyme solutions without Aβ microfibrils were subtracted from the spectra, and four scans were averaged. Data are expressed as molar residue ellipticities using 42 and 0.3 mM as the number of amino acids and the concentration, respectively. The contents of secondary structure elements of Aβ peptides were estimated by published methods (*32*).

Cell Viability Assay. The Aβ microfibrils were degraded by protease XIV and α-chymotrypsin for 24 h at 37 °C, and parts of them were filtered with a Microncon 10000 MWCO (Millipore Corp.). Also, the Aβ microfibrils were degraded by NEP and IDE for 48 h at 37 °C. The overall and filtered degradation products were added to 96-well plates to yield final concentrations of Aβ peptides of 27.5, 55, 110, and 220 μg/mL. The concentrations of the samples were determined from UV measurement (diode array spectrophotometer 8452A, Hewlett-Packard, Palo Alto, CA) using absorption at 280 nm dependent on Phe and Tyr. The enzyme solutions were used as background to determine the concentration of Aβ peptides. Rat pheochromocytoma (PC12) cells were differentiated in medium (F-12K, 0.5% FBS, 100 μM nerve growth factor) and maintained for 24 h at 37 °C in an atmosphere of 5% CO_2. For the cell viability assay, cells were plated in the 96-well plates at a density of 30000 cells per well and maintained in the medium. Cells were incubated with the Aβ microfibrils and their degradation products for 24 h, and then cell viability was measured with a CellTiter 96 AQueous Non-Radioactive Cell Proliferation Assay {MTS [3-(4,5-dimethylthiazol-2-yl)-5-(3-carboxymethoxyphenyl)-2-(4-sulfophenyl)-2*H*-tetrazolium] (*33*); Promega, Madison, WI}, according to the manufacturer's protocol.

Statistical Analysis. Statistical differences in cell viability were determined with an unpaired *t* test with a two-tailed distribution, and differences were considered statistically significant at $p < 0.05$. The data in the cell viability experiments are expressed as means ± the standard deviation ($n = 8$).

RESULTS AND DISCUSSION

Characterization of Aβ Microfibrils. An Aβ(1−42) solution was prepared by dissolving Aβ(1−42) peptide in DMSO and 10 mM HCl, followed by incubation at 37 °C for 2 days, to produce Aβ microfibrils (*4*, *29*). The Aβ microfibrils were characterized by optical microscopy (OM), atomic force microscopy (AFM), and microscopic Fourier transform infrared spectroscopy (MFTIR). OM and AFM amplitude images of Aβ microfibrils are shown in Figure 1, and the microfibrils were composed of several nanofibrils (Figure 1D). The thickness and width of the nanofibrils were approximately 7 and 30 nm, respectively (Figure 1E). To determine the fraction of secondary structure of the microfibrils in air, MFTIR spectra were recorded and deconvoluted in the amide I region (Figure S1 of the Supporting Information), resulting in the Aβ microfibrils containing 71 ± 8% β-sheet, 12 ± 2% α-helix and

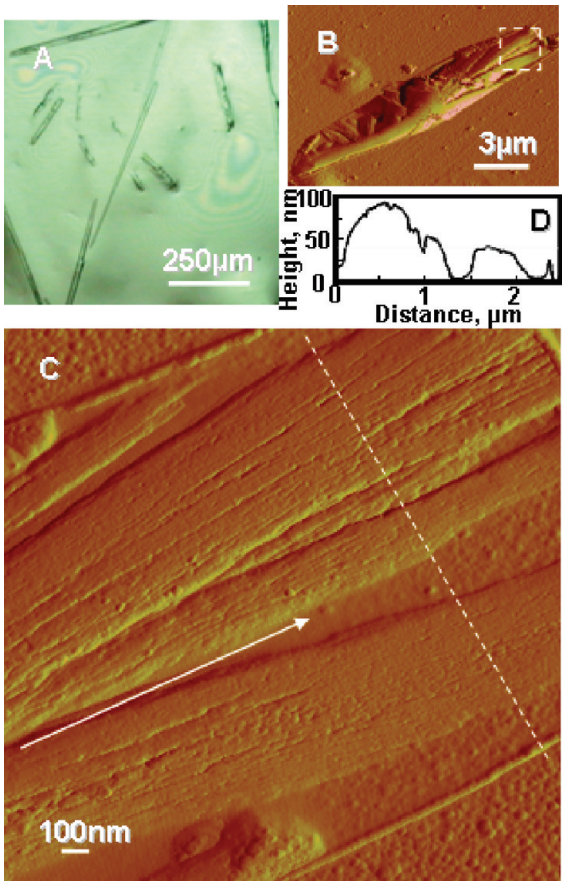

FIGURE 1: Aβ fibrils before enzymatic degradation. (A) Optical microscopy image of Aβ fibrils. (B) Typical AFM amplitude image of an Aβ microfibril. (C) Enlargement of boxed area in panel B. Nanofibrils composing the microfibril are aligned along a white arrow. (D) Line profile data of the fibrils marked with a white dashed line in panel C.

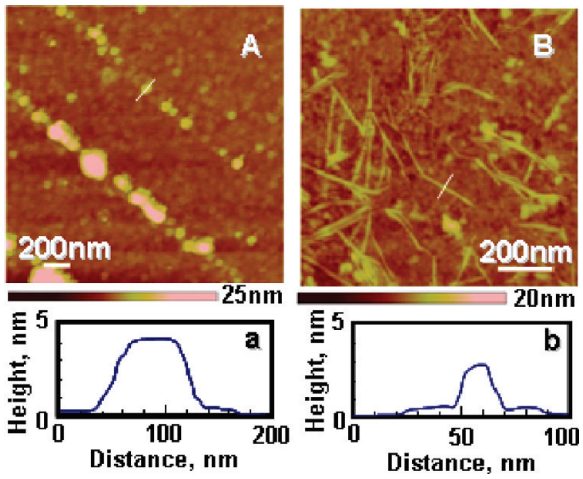

FIGURE 2: Aβ fibrils after enzymatic degradation for 24 h. AFM height images of Aβ fibrils during enzymatic degradation by protease XIV (A) and by α-chymotrypsin (B). Panels a and b show line profile data of the crystals indicated by the white lines in panels A and B.

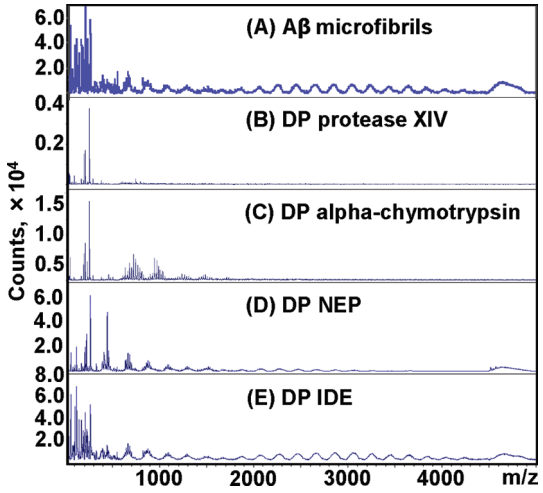

FIGURE 3: Enzymatic digestion patterns of Aβ fibrils. MALDI-TOF analysis of Aβ fibrils before (A) and after enzymatic degradation for 24 h by protease XIV (B) and α-chymotrypsin (C) and for 48 h by NEP (D) and IDE (E).

random coil, and 17 ± 5% turns based on the previous assignments (*34*, *35*). Thus, the Aβ microfibrils prepared for our study were composed of nanofibrils with a high-β-sheet content structure.

Enzymatic Degradation of Aβ Microfibrils. Protease XIV, α-chymotrypsin, NEP, and IDE, previously reported to degrade β-sheet structures or soluble Aβ peptides, were used as Aβ-degrading enzymes in this study (*16*−*24*). AFM observations of the Aβ microfibrils were performed after enzymatic degradation over 24 h by protease XIV or α-chymotrypsin (Figure 2). Protease XIV and α-chymotrypsin at the same concentration as in the degradation experiments without Aβ peptides were also observed by AFM as negative controls (Figure S2 of the Supporting Information). The Aβ microfibrils exposed to the protease XIV exhibited spherical degradation products that were 50−100 nm in width and 4−10 nm in height (Figure 2A). Several research groups have reported spherical morphologies such as oligomers (~5 nm in diameter), amylospheroids (8−16 nm), and intermediates (15−35 nm) (*5*, *36*, *37*). The spherical morphologies of the degradation products from protease XIV are similar to those of the intermediates reported previously in terms of dimensions (*5*). In contrast, α-chymotrypsin degraded the Aβ microfibrils into fibril-like fragments (nanofilaments) that were ~20 nm in width and 3 nm in height (Figure 2B), indicating that the Aβ microfibrils used in this study contained crystalline nanofilaments that cannot be degraded by α-chymotrypsin. The nanofilaments from α-chymotrypsin are very similar to Aβ paired helical filaments with the cross-β conformation that were observed in the frozen cerebral cortex of AD patients (*38*). On the basis of the dimensions of nanofilaments observed, as well as the crystal structure of cross-β Aβ (*39*, *40*), the nanofilaments may be composed of two cross-β units along the thickness (perpendicular to the fiber axis). The Aβ microfibrils exposed to NEP and IDE for 48 h exhibited almost no significant degradation, suggesting a relatively low degrading activity of these enzymes against crystalline (solid-state) Aβ peptides (Figure S3 of the Supporting Information). NEP and IDE are therefore supposed to digest preferentially soluble monomeric Aβ peptides on the basis of previous reports that IDE exhibits a significantly lower degradation activity with respect to dimeric Aβ in comparison with monomeric Aβ (*41*−*43*).

To reveal the enzymatic digestion pattern of each Aβ peptide that was composed the Aβ microfibrils, the Aβ microfibrils and their degradation products at 24 h (protease XIV and α-chymotrypsin) and 48 h (NEP and IDE) were characterized by MALDI-TOF (Figure 3). Protease XIV and α-chymotrypsin at the same concentration as the degradation products without Aβ peptides were also characterized by MALDI-TOF as negative

controls (Figure S4 of the Supporting Information). Proteases generally degrade themselves, resulting in many degradation fragments. Amino acid sequences of the degradation products were evaluated; however, it was difficult to clarify these by MALDI-TOF because of the many peaks from the proteases themselves, as shown in Figure S4 of the Supporting Information. The Aβ microfibrils prepared in this study contained several low-molecular weight (< 2000) fragments in addition to full-length Aβ(1−42) peptides (4514) (Figure 3A). The low-molecular weight fragments in the Aβ microfibrils could be products of degradation by acids used for the preparation of Aβ microfibrils. The degradation products from protease XIV contained no full-length Aβ(1−42) peptides but low-molecular weight (< 1000) fragments (Figure 3B), indicating that protease XIV digested several sites of Aβ(1−42). In contrast, the degradation products from α-chymotrypsin exhibited several higher-molecular weight (500−1500 Da) components as well as no full-length Aβ(1−42) peptides (Figure 3C), implying that α-chymotrypsin digested fewer sites of Aβ(1−42) in comparison to protease XIV. Although NEP and IDE provided several low-molecular weight fragments, the full-length Aβ(1−42) peptides remained (Figure 3D,E). The numerous peaks between m/z 1000 and 4000 in panels D and E of Figure 3 originated from the degradation products by acids used for the preparation of Aβ microfibrils, as shown in Figure 3A. These results also support the relatively low degrading activity of NEP and IDE against crystalline Aβ(1−42) peptides.

Protease XIV and α-chymotrypsin are serine esterases that hydrolyze preferentially peptide bonds to the C-terminal side of aromatic amino acids (*26*−*28*). We estimated the digestion patterns of an Aβ(1−42) molecule with a random-coil structure by protease XIV or α-chymotrypsin, according to the substrate specificity of the enzymes and the molecular weights of degradation products by MALDI-TOF (Figure 4A) (*26*−*28*). Thus, enzymatic digestion patterns of random-coil Aβ(1−42) molecules by protease XIV and α-chymotrypsin were nearly identical except for that of Lys28. The digestion of Lys28, which means the digestion of the loop region linking two β-sheets (β1 and β2), is a significant difference in the pattern of digestion between the two enzymes (Figure 4A), since the digestion of Lys28 must induce the degradation of the β-hairpin structure of Aβ molecules (Figure 4B,C). This difference in predicted digestion patterns of Aβ molecules could influence the structure of degradation products. Also, protease XIV exhibited degradation activity toward the crystalline β-sheets, whereas α-chymotrypsin was not capable of digesting crystalline β-sheets (*22*−*24*). Therefore, we suggest that protease XIV-digested Lys28 of the Aβ crystalline region and the cross-β structure could be degraded into the spherical products that were 50−100 nm in width and 4−10 nm in height (Figure 2A), while α-chymotrypsin could not digest the Lys28 in the crystalline region, resulting that the nanofilament with β-sheet structure retained. The nanofilaments could also consist mainly of hairpin structures from Gln15 to Ala42 on the basis of the digestion patterns, crystal structures, and results from MALDI measurements (Figure 3C).

To determine the secondary structure of Aβ molecules before and after enzymatic degradation, we performed circular dichroism (CD) analyses of overall and filtered (10K MWCO) samples of the Aβ microfibrils and their degradation products by protease XIV, α-chymotrypsin, NEP, or IDE. The CD spectrum of all samples exhibited β-sheet structure with a negative shoulder at 216 nm (Figure 5). Estimation of the secondary structure

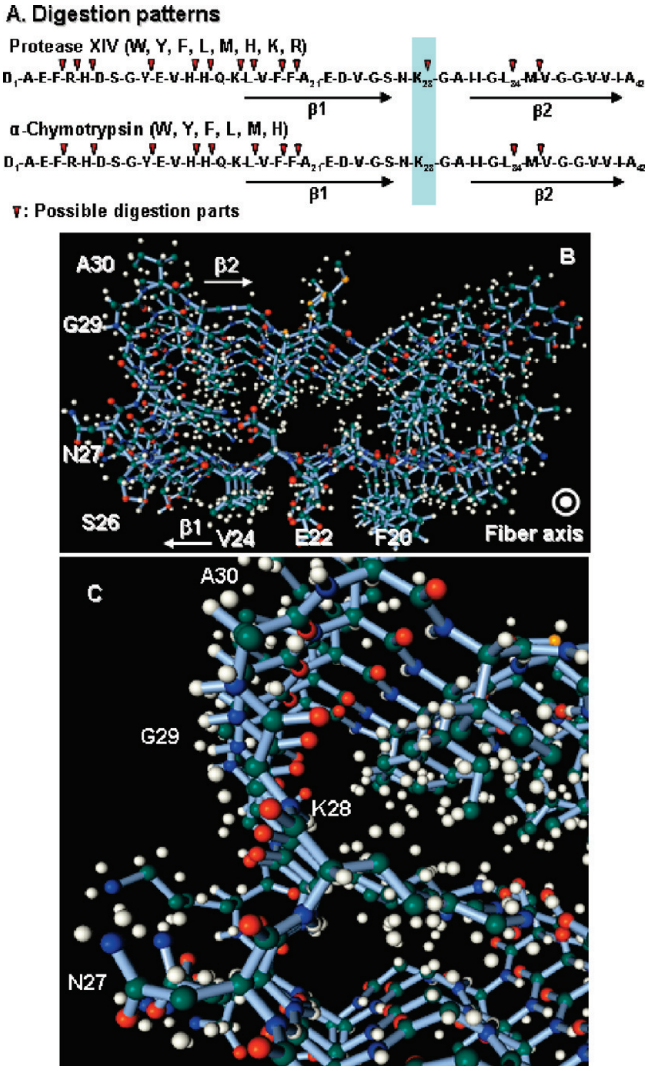

FIGURE 4: Model of enzymatic digestion and crystal structures of Aβ. (A) Enzymatic digestion patterns estimated on the basis of the enzymatic specificities. (B) Structure of the 5mer of Aβ(1−42) peptides with cross-β structure. (C) Enlargement of cross-β structure around K28 in panel B. The data of panels B and C were obtained from Protein Data Bank entry 2beg and processed with Facio version 12.1.2 (*33*).

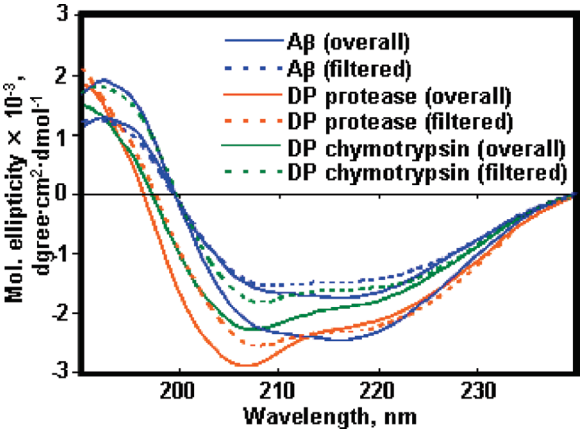

FIGURE 5: CD analyses of the Aβ fibrils before and after enzymatic degradation for 24 h. Blue solid and dotted lines show data for the overall and filtered Aβ fibril solution before enzymatic degradation. Green and orange solid and dotted lines show data for the overall and filtered degradation products (DP) by protease XIV and α-chymotrypsin, respectively.

contents of the overall Aβ microfibrils and degradation products from protease XIV, α-chymotrypsin, NEP, and IDE yielded 37 ± 5, 30 ± 8, 33 ± 9, 42 ± 9, and 47 ± 10% β-strand structures, respectively (Table S1 of the Supporting Information). In the case of the filtered samples, the secondary structures of Aβ microfibrils, degradation products from protease XIV, and degradation products from α-chymotrypsin were estimated to be 18 ± 3, 13 ± 2, and 14 ± 4% β-strand structures, respectively. The spherical degradation products from protease XIV and the nanofilaments from α-chymotrypsin were removed by filtration (10K MWCO); therefore, the filtered samples contained no nanoassembled degradation products, only water-soluble Aβ peptides. The overall degradation products from protease XIV and α-chymotrypsin exhibited higher β-strand content than the filtered degradation products. The differences in β-strand structure content between the samples before and after filtration were the cause of these nanoassembled degradation products, which were removed by the filter. The overall degradation products from NEP and IDE exhibited higher β-strand contents in comparison to the overall Aβ microfibrils, indicating that these enzymes degraded preferentially noncrystalline regions of Aβ.

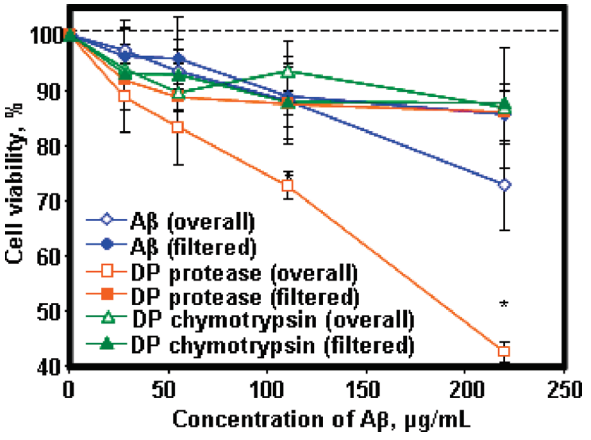

FIGURE 6: Cell viability with the Aβ fibrils and their degradation fragments on differentiated PC12 cells. Dependence of cell viability (percentage of active cells as compared to controls) on the Aβ peptides measured by the MTS assay. Overall Aβ fibrils (blue diamonds) exhibit cell viability percentages of Aβ fibrils before enzymatic degradation. Filtered soluble Aβ fragments (blue diamonds) exhibit cell viability percentages of filtered Aβ fibrils before enzymatic degradation. Overall degradation products (DP) of protease XIV (filled orange squares) and α-chymotrypsin (filled green triangles) show the percentages of each degradation product. Filtered soluble DP produced by protease XIV (empty orange squares) and α-chymotrypsin (empty green triangles) show the percentages of each filtered degradation product. Data are represented as means ± the standard deviation (n = 8). The asterisk denotes a significant difference between two groups ($p < 0.05$).

Cytotoxicity of Degradation Products. The Aβ microfibrils and their products of degradation by protease XIV, α-chymotrypsin, NEP, and IDE were evaluated for neurotoxicity to differentiated Rat pheochromocytoma (PC12) cells using the MTS assay. The overall and filtered Aβ microfibrils before enzymatic degradation and degradation products after 24 h from protease XIV and α-chymotrypsin were tested at 27.5, 55, 110, and 220 μg/mL (Figure 6). All the filtered samples showed no significant cytotoxicity to neuronal cells up to the highest concentration used in this study. Also, protease XIV and α-chymotrypsin (100 μg/mL) incubated for 24 h at 37 °C showed no cytotoxicity, with cell viabilities of 105 ± 9 and 110 ± 12%, respectively. The overall degradation products from α-chymotrypsin demonstrated no significant cytotoxicity, while the overall Aβ microfibrils and degradation products from protease XIV exhibited lower cell viability in comparison to the other samples. On the basis of these cell viability results, soluble Aβ fragments, which were filtered from the degradation products, as well as the overall degradation products with 33 ± 9% β-sheet structure from α-chymotrypsin containing the nanofilaments, showed no cytotoxicity. On the other hand, the overall degradation products with 30 ± 8% β-sheet structures from protease XIV digestion had a significant impact on PC12 cells, indicating that the spherical degradation products were cytotoxic. The cells after the incubation with the overall degradation products from protease XIV digestion were observed by OM as shown in Figure S5 of the Supporting Information. The overall degradation products from NEP and IDE showed the same cytotoxicity to the overall Aβ microfibrils before enzymatic degradation (Figure S6 of the Supporting Information), even though the average β-sheet contents of degradation products from NEP and IDE (42 ± 9 and 47 ± 10%, respectively) were slightly higher than the overall content of Aβ microfibrils (37 ± 5%). IDE was reported to be able to enzymatically process the Aβ, yielding new fragments that are not neurotoxic or that do not deposit on amyloid plaques (*44*, *45*). The difference in cytotoxicity and β-sheet content indicates that the factor that determines cytotoxicity is the amino acid sequence of Aβ peptides, yielding nanoassembled structures, rather than just the β-sheet content of Aβ peptides. In any of the assessments described above, in vivo studies would be required to more fully discern the importance of sequence chemistry and fragment composition with respect to toxicity.

Mechanism of Enzymatic Degradation of Aβ Related to Cytotoxicity. On the basis of our results, we propose a model of enzymatic degradation of cross-β Aβ due to protease activity (Figure 7): the typical cross-β structure, which is in-register parallel alignment in the cross-β motif with N-terminal disorder, is presented in Figure 7A, according to X-ray diffraction and NMR data (*39*, *40*, *46*, *47*). Taking into account the digestion

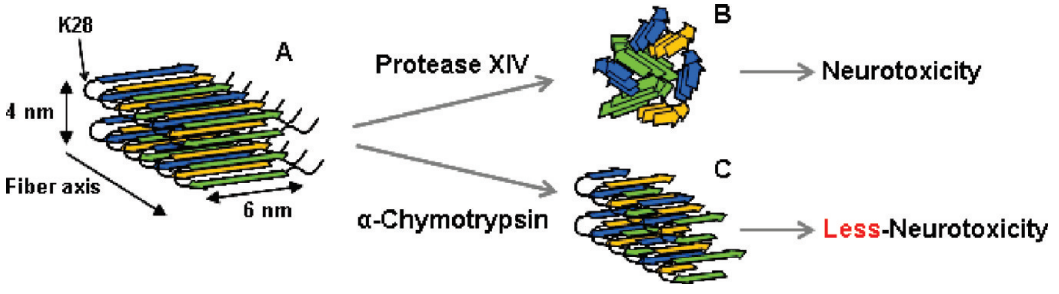

FIGURE 7: Models of the enzymatic reaction of Aβ fibrils in nanometer scale by protease XIV and α-chymotrypsin. (A) Aβ with cross-β structure, (B) spherical degradation products from protease XIV, and (C) nanofilaments from α-chymotrypsin.

patterns of proteolytic enzymes, we found that the Lys28 at the loop region is digested by protease XIV and the β-strand structures assemble with each other randomly into the spherical degradation products via hydrophobic interactions (Figure 7B). This spherical assembly of β-strands causes neurotoxicity to cells. In contrast, α-chymotrypsin is not capable of digesting the loop region to link two β-sheets in the crystalline region, and therefore, some parts of the Aβ crystal structure, such as nanofilaments, are maintained (Figure 7C). According to the crystal structure, the dimensions of one pair of Aβ hairpins are around 6 nm wide and 4 nm thick (*39*, *40*). In this study, the width and thickness of nanofilaments were approximately 20 and 3 nm, respectively. Hence, a nanofilament consists of one pair and a few Aβ hairpins along the thickness and width, judging from the dimensions observed by AFM.

The degradation products from α-chymotrypsin including nanofilaments show no significant cytotoxicity to PC12 cells. The difference between two degradation products, nanospheres and nanofilaments, is due to not only the structural morphologies but also the presence of Aβ fragments that have Lys at their chain ends. The Aβ fragments with Lys28 at the N-terminus have been reported to be more toxic than the other Aβ fragments, because of the charged Lys (*7*). Plasmin not only digested Aβ aggregates but also protected neurons from Aβ toxicity (*48*, *49*). Six of eight degradation fragments from plasmin contained Lys at the C-terminus (*48*). On the basis of these results and the literature (*7*, *48*), Lys28 is a feasible key to collapsing the cross-β structure, and moreover, Lys at the N-terminus has a significant role in the neurotoxicity of Aβ peptides. The β-sheet content of Aβ peptides is one of the main factors related to neurotoxicity. In addition, the nanoassembled structure of Aβ may also be a key element in terms of neurotoxicity.

The degradation model described provides new views concerning the fundamental mechanisms of enzymatic responses of Aβ fibrils as well as Aβ nanoassembly related to neurotoxicity. We identified nanofilaments around 3 nm thick and 20 nm wide, which did not exhibit significant cytotoxicity, during enzymatic degradation of the Aβ fibrils. The spherical degradation products observed during enzymatic degradation demonstrated significant toxicity. As mentioned above, relationships between nanoassembled structures of Aβ and their cytotoxicity are also suggested, which means nanoassembled structures rather than the β-sheet content of disease proteins can be a more significant factor in exhibiting cytotoxicity. Also, the digestion of Lys28 at the loop region to link two β-sheets of Aβ fibrils is suggested to generate significant cytotoxicity to cells. This finding provides an opportunity to avoid cytotoxicity when Aβ fibrils are enzymatically digested to reduce the level of accumulation of Aβ in the brain. For instance, Aβ fibrils and plaques could be degraded without significant cytotoxicity by inhibiting digestion of the loop region with antibodies. Furthermore, this new insight provides options for addressing structural mechanisms of amyloids for various disease proteins as well as AD therapeutics with enzymatic treatments.

SUPPORTING INFORMATION AVAILABLE

Additional data (Table S1 and Figures S1−S6). This material is available free of charge via the Internet at http://pubs.acs.org.

REFERENCES

1. Selkoe, D. J. (2003) Folding proteins in fatal ways. *Nature 426*, 900–904.
2. Ross, C. A., and Poirier, M. A. (2005) Opinion: What is the role of protein aggregation in neurodegeneration? *Nat. Rev. Mol. Cell Biol. 6*, 891–898.
3. Sipe, J. D., and Cohen, A. S. (2000) History of the amyloid fibril. *J. Struct. Biol. 130*, 88–98.
4. Nagai, Y., Inui, T., Popiel, H. A., Fujikake, N., Hasegawa, K., Urade, Y., Goto, Y., Naiki, H., and Toda, T. (2007) A toxic monomeric conformer of the polyglutamine protein. *Nat. Struct. Mol. Biol. 14*, 332–340.
5. Chimon, S., Shaibat, M. A., Jones, C. R., Calero, D. C., Aizezi, B., and Ishii, Y. (2007) Evidence of fibril-like β-sheet structures in a neurotoxic amyloid intermediate of Alzheimer's β-amyloid. *Nat. Struct. Mol. Biol. 14*, 1157–1164.
6. Jarrett, J. T., Berger, E. P., and Lansbury, P. T., Jr. (1993) The carboxy terminus of the β amyloid protein is critical for the seeding of amyloid formation: Implications for the pathogenesis of Alzheimer's disease. *Biochemistry 32*, 4693–4697.
7. Fradinger, E. A., Monien, B. H., Urbanc, B., Lomakin, A., Tan, M., Li, H., Spring, S. M., Condron, M. M., Cruz, L., Xie, C. W., Benedek, G. B., and Bitan, G. (2008) C-Terminal peptides coassemble into Aβ42 oligomers and protect neurons against Aβ42-induced neurotoxicity. *Proc. Natl. Acad. Sci. U.S.A. 105*, 14175–14180.
8. Yatin, S. M., Varadarajan, S., Link, C. D., and Butterfield, D. A. (1999) In vitro and in vivo oxidative stress associated with Alzheimer's amyloid β-peptide (1−42). *Neurobiol. Aging 20*, 325–330.
9. Drake, J., Link, C. D., and Butterfield, D. A. (2003) Oxidative stress precedes fibrillar deposition of Alzheimer's disease amyloid β-peptide (1−42) in a transgenic *Caenorhabditis elegans* model. *Neurobiol. Aging 24*, 415–420.
10. Citron, M. (2004) Strategies for disease modification in Alzheimer's disease. *Nat. Rev. Neurosci. 5*, 677–685.
11. Masliah, E., Hansen, L., Adame, A., Crews, L., Bard, F., Lee, C., Seubert, P., Games, D., Kirby, L., and Schenk, D. (2005) Aβ vaccination effects on plaque pathology in the absence of encephalitis in Alzheimer's disease. *Neurology 64*, 129–131.
12. Schenk, D., Barbour, R., Dunn, W., Gordon, G., Grajeda, H., Guido, T., Hu, K., Huang, J., Johnson-Wood, K., Khan, K., Kholodenko, D., Lee, M., Liao, Z., Lieberburg, I., Motter, R., Mutter, L., Soriano, F., Shopp, G., Vasquez, N., Vandevert, C., Walker, S., Wogulis, M., Yednock, T., Games, D., and Seubert, P. (1999) Immunization with amyloid-β attenuates Alzheimer-disease-like pathology in the PDAPP mouse. *Nature 400*, 173–177.
13. Iwata, N., Tsubuki, S., Takaki, Y., Watanabe, K., Sekiguchi, M., Hosoki, E., Kawashima-Morishima, M., Lee, H. J., Hama, E., Sekine-Aizawa, Y., and Saido, T. C. (2000) Identification of the major Aβ1−42-degrading catabolic pathway in brain parenchyma: Suppression leads to biochemical and pathological deposition. *Nat. Med. 6*, 143–150.
14. Madani, R., Poirier, R., Wolfer, D. P., Welzl, H., Groscurth, P., Lipp, H. P., Lu, B., El Mouedden, M., Mercken, M., Nitsch, R. M., and Mohajeri, M. H. (2006) Lack of neprilysin suffices to generate murine amyloid-like deposits in the brain and behavioral deficit in vivo. *J. Neurosci. Res. 84*, 1871–1878.
15. Authier, F., Posner, B. I., and Bergeron, J. J. (1996) Insulin-degrading enzyme. *Clin. Invest. Med. 19*, 149–160.
16. Duckworth, W. C., Bennett, R. G., and Hamel, F. G. (1998) Insulin degradation: Progress and potential. *Endocr. Rev. 19*, 608–624.
17. Pardossi-Piquard, R., Dunys, J., Yu, G., St George-Hyslop, P., Alves da Costa, C., and Checler, F. (2006) Neprilysin activity and expression are controlled by nicastrin. *J. Neurochem. 97*, 1052–1056.
18. Leissring, M. A., Farris, W., Wu, X., Christodoulou, D. C., Haigis, M. C., Guarente, L., and Selkoe, D. J. (2004) Alternative translation initiation generates a novel isoform of insulin-degrading enzyme targeted to mitochondria. *Biochem. J. 383*, 439–446.
19. Ciaccio, C., Tundo, G. R., Grasso, G., Spoto, G., Marasco, D., Ruvo, M., Gioia, M., Rizzarelli, E., and Coletta, M. (2009) Somatostatin: A novel substrate and a modulator of insulin-degrading enzyme activity. *J. Mol. Biol. 385*, 1556–1567.
20. Song, E. S., Juliano, M. A., Juliano, L., and Hersh, L. B. (2003) Substrate activation of insulin-degrading enzyme (insulysin). A potential target for drug development. *J. Biol. Chem. 278*, 49789–49794.
21. Arai, T., Freddi, G., Innocenti, R., and Tsukada, M. (2004) Biodegradation of *Bombyx mori* silk fibroin fibers and films. *J. Appl. Polym. Sci. 91*, 2383–2390.
22. Lotz, B., Gonthier-Vassal, A., Brack, A., and Magoshi, J. (1982) Twisted single crystals of *Bombyx mori* silk fibroin and related model polypeptides with β structure. A correlation with the twist of the β sheets in globular proteins. *J. Mol. Biol. 156*, 345–357.

23. Li, M., Ogiso, M., and Minoura, N. (2003) Enzymatic degradation behavior of porous silk fibroin sheets. *Biomaterials 24*, 357–365.
24. Numata, K., Cebe, P., and Kaplan, D. L. (2010) Mechanism of enzymatic degradation of β-sheet crystals. *Biomaterials 31*, 2926–2933.
25. Horan, R. L., Antle, K., Collette, A. L., Wang, Y., Huang, J., Moreau, J. E., Volloch, V., Kaplan, D. L., and Altman, G. H. (2005) In vitro degradation of silk fibroin. *Biomaterials 26*, 3385–3393.
26. Bauer, C. A., Thompson, R. C., and Blout, E. R. (1976) The active centers of *Streptomyces griseus* protease 3 and α-chymotrypsin: Enzyme-substrate interactions remote from the scissile bond. *Biochemistry 15*, 1291–1295.
27. Bauer, C. A., Thompson, R. C., and Blout, E. R. (1976) The active centers of *Streptomyces griseus* protease 3, α-chymotrypsin, and elastase: Enzyme-substrate interactions close to the scissile bond. *Biochemistry 15*, 1296–1299.
28. Bauer, C. A. (1978) Active centers of *Streptomyces griseus* protease 1, *Streptomyces griseus* protease 3, and α-chymotrypsin: Enzyme-substrate interactions. *Biochemistry 17*, 375–380.
29. Stine, W. B., Jr., Dahlgren, K. N., Krafft, G. A., and LaDu, M. J. (2003) In vitro characterization of conditions for amyloid-β peptide oligomerization and fibrillogenesis. *J. Biol. Chem. 278*, 11612–11622.
30. Numata, K., Hirota, T., Kikkawa, Y., Tsuge, T., Iwata, T., Abe, H., and Doi, Y. (2004) Enzymatic degradation processes of lamellar crystals in thin films for poly[(R)-3-hydroxybutyric acid] and its copolymers revealed by real-time atomic force microscopy. *Biomacromolecules 5*, 2186–2194.
31. Kanemitsu, H., Tomiyama, T., and Mori, H. (2003) Human neprilysin is capable of degrading amyloid β peptide not only in the monomeric form but also the pathological oligomeric form. *Neurosci. Lett. 350*, 113–116.
32. Sreerama, N., and Woody, R. W. (1993) A self-consistent method for the analysis of protein secondary structure from circular dichroism. *Anal. Biochem. 209*, 32–44.
33. Riss, T. L., and Moravec, R. A. (1992) Comparison of MTT, XTT, and a novel tetrazolium compound for MTS for in vitro proliferation and chemosensitivity assays. *Mol. Biol. Cell 3*, 184a.
34. Cheatum, C. M., Tokmakoff, A., and Knoester, J. (2004) Signatures of β-sheet secondary structures in linear and two-dimensional infrared spectroscopy. *J. Chem. Phys. 120*, 8201–8215.
35. Rak, M., Del Bigio, M. R., Mai, S., Westaway, D., and Gough, K. (2007) Dense-core and diffuse Aβ plaques in TgCRND8 mice studied with synchrotron FTIR microspectroscopy. *Biopolymers 87*, 207–217.
36. Lambert, M. P., Barlow, A. K., Chromy, B. A., Edwards, C., Freed, R., Liosatos, M., Morgan, T. E., Rozovsky, I., Trommer, B., Viola, K. L., Wals, P., Zhang, C., Finch, C. E., Krafft, G. A., and Klein, W. L. (1998) Diffusible, nonfibrillar ligands derived from Aβ1−42 are potent central nervous system neurotoxins. *Proc. Natl. Acad. Sci. U.S.A. 95*, 6448–6453.
37. Hoshi, M., Sato, M., Matsumoto, S., Noguchi, A., Yasutake, K., Yoshida, N., and Sato, K. (2003) Spherical aggregates of β-amyloid (amylospheroid) show high neurotoxicity and activate tau protein kinase I/glycogen synthase kinase-3β. *Proc. Natl. Acad. Sci. U.S.A. 100*, 6370–6375.
38. Kirschner, D. A., Abraham, C., and Selkoe, D. J. (1986) X-ray diffraction from intraneuronal paired helical filaments and extraneuronal amyloid fibers in Alzheimer disease indicates cross-β conformation. *Proc. Natl. Acad. Sci. U.S.A. 83*, 503–507.
39. Petkova, A. T., Ishii, Y., Balbach, J. J., Antzutkin, O. N., Leapman, R. D., Delaglio, F., and Tycko, R. (2002) A structural model for Alzheimer's β-amyloid fibrils based on experimental constraints from solid state NMR. *Proc. Natl. Acad. Sci. U.S.A. 99*, 16742–16747.
40. Lührs, T., Ritter, C., Adrian, M., Riek-Loher, D., Bohrmann, B., Döbeli, H., Schubert, D., and Riek, R. (2005) 3D structure of Alzheimer's amyloid-β(1−42) fibrils. *Proc. Natl. Acad. Sci. U.S.A. 102*, 17342–17347.
41. Morelli, L., Llovera, R., Gonzalez, S. A., Affranchino, J. L., Prelli, F., Frangione, B., Ghiso, J., and Castano, E. M. (2003) Differential degradation of amyloid β genetic variants associated with hereditary dementia or stroke by insulin-degrading enzyme. *J. Biol. Chem. 278*, 23221–23226.
42. Morelli, L., Llovera, R. E., Alonso, L. G., Frangione, B., de Prat-Gay, G., Ghiso, J., and Castaño, E. M. (2005) Insulin-degrading enzyme degrades amyloid peptides associated with British and Danish familial dementia. *Biochem. Biophys. Res. Commun. 332*, 808–816.
43. Zhao, J., Li, L., and Leissring, M. A. (2009) Insulin-degrading enzyme is exported via an unconventional protein secretion pathway. *Mol. Neurodegener. 4*, 4.
44. Chesneau, V., Vekrellis, K., Rosner, M. R., and Selkoe, D. J. (2000) Purified recombinant insulin-degrading enzyme degrades amyloid β-protein but does not promote its oligomerization. *Biochem. J. 351* (Part 2), 509–516.
45. Mukherjee, A., Song, E., Kihiko-Ehmann, M., Goodman, J. P., Jr., Pyrek, J. S., Estus, S., and Hersh, L. B. (2000) Insulysin hydrolyzes amyloid β peptides to products that are neither neurotoxic nor deposit on amyloid plaques. *J. Neurosci. 20*, 8745–8749.
46. Inouye, H., Fraser, P. E., and Kirschner, D. A. (1993) Structure of β-crystallite assemblies formed by Alzheimer β-amyloid protein analogues: Analysis by X-ray diffraction. *Biophys. J. 64*, 502–519.
47. Malinchik, S. B., Inouye, H., Szumowski, K. E., and Kirschner, D. A. (1998) Structural analysis of Alzheimer's β(1−40) amyloid: Protofilament assembly of tubular fibrils. *Biophys. J. 74*, 537–545.
48. Tucker, H. M., Kihiko, M., Caldwell, J. N., Wright, S., Kawarabayashi, T., Price, D., Walker, D., Scheff, S., McGillis, J. P., Rydel, R. E., and Estus, S. (2000) The plasmin system is induced by and degrades amyloid-β aggregates. *J. Neurosci. 20*, 3937–3946.
49. Jacobsen, J. S., Comery, T. A., Martone, R. L., Elokdah, H., Crandall, D. L., Oganesian, A., Aschmies, S., Kirksey, Y., Gonzales, C., Xu, J., Zhou, H., Atchison, K., Wagner, E., Zaleska, M. M., Das, I., Arias, R. L., Bard, J., Riddell, D., Gardell, S. J., Abou-Gharbia, M., Robichaud, A., Magolda, R., Vlasuk, G. P., Bjornsson, T., Reinhart, P. H., and Pangalos, M. N. (2008) Enhanced clearance of Aβ in brain by sustaining the plasmin proteolysis cascade. *Proc. Natl. Acad. Sci. U.S.A. 105*, 8754–8759.